

THERMALLY-INDUCED DEPOLARIZATION CURRENT SPECTRA OF NaCl:Ni²⁺ CRYSTALS

M. SUSZYŃSKA

W. Trzebiatowski Institute of Low Temperature and Structure Research
Polish Academy of Sciences, Pl. Katedralny 1, 50-950 Wrocław, Poland

AND R. CAPELLETTI

Physics Department, Parma University, Parma, Italy

(Received June 3, 1991; in final form July 29, 1991)

The technique of thermally stimulated depolarization currents was exploited to search dipolar defects in NaCl crystals doped with divalent nickel in a wide concentration range. The results were critically compared with those typical of other impurities. It has been shown that the main features of the detected polarizations are qualitatively similar to those characteristic of alkali halides doped with divalent cations. The differences observed in some instances can be understood in terms of different mobility and/or stability of the elementary defects related with the impurities.

PACS numbers: 77.40.+i

1. Introduction

Most of the divalent ions (Me^{2+}) are introduced into alkali halides (AH) substitutionally, and per each impurity ion one cation vacancy is also introduced. If the temperature is not too high, both species form the impurity-vacancy (I.V.) dipoles. For increasing dopant concentration these dipoles undergo aggregation and form higher clusters which may be or may be not endowed in a dipolar moment.

Among the methods used in investigations of the dipolar defects in ionic crystals is that one based on the measurements of thermally-induced depolarization currents (ITC); this method was originally developed by Bucci et al. [1]. For simple I.V. dipoles, with a known dipole moment, the measured ITC-spectrum yields the following data:

- the concentration of dipolar defects,
- the mechanism of reorientation of these defects in the electric field, and
- the parameters characterizing the temperature-dependence of the relaxation time τ , i.e. the activation energy E and the frequency factor τ_0^{-1} .

On the other hand, more complex defects may also result in the appearance of some ITC bands positioned at and above room temperature (RT). It has been shown previously [2, 3] that some of these bands are explainable in terms of Maxwell-Wagner-Sillars theory of polarization in heterogeneous dielectrics [4]. Hence, studies of the behaviour of these bands can yield important information concerning the morphology and/or structure of the related defects.

The purpose of the experiments described in this paper was to obtain information concerning the behaviour and/or features of all reorientable defects present in NaCl crystals doped with divalent nickel ions. It should be noted that the ionic radius of Ni^{2+} ions is distinctly smaller than that of the matrix cation. In such crystal systems there are additional possibilities for the location of both the impurity (besides the substitution) as well as the excess-charge compensating cation vacancies (besides the nearest-neighbour-one). Namely, one has to consider the interstitial and off-centre positions for the impurity as well as the next-nearest-neighbour-site for the vacancy. Some considerations of these problems can be found for AgCl with Fe^{2+} [5], NaCl and KCl with Be^{2+} [6], and — more generally — for the AH crystals doped with Me^{2+} cations of different size [7–9].

The results obtained were, among others, critically compared with those obtained previously [3] for NaCl and KCl crystals doped with Pb^{2+} and Eu^{2+} ions.

2. Experimental details

2.1. Crystal samples

The NaCl: Ni^{2+} crystals have been either grown in our laboratory or purchased from the Laboratories mentioned in Table I. All crystals were grown according to the Bridgman method with some modifications diminishing the contamination by oxygen-containing anions [10].

Concentration of the dopant was determined from the optical absorption measurements by using the relationship between the absorption coefficient $\alpha(C)$ of the main absorption band and the dopant concentration c_{2+} ; for $\alpha(C)$ expressed in cm^{-1} and c_{2+} in mole ppm, $A \equiv c_{2+}/\alpha(C) = 1.78$ [11].

The measurements were performed for as-received (AR) and solution treated (ST) samples, where the solution treatment of AR samples comprised 30 minutes of annealing at 873 K and the quenching to RT by putting the hot sample on a copper plate.

Two kinds of samples were used, namely:

- for the conventional ITC measurements — plates about 1 cm^2 in cross section and about 1 mm thick;
- for measurements performed after plastic deformation (uniaxial compression in a self-made device) — parallelepipeds of approximate size $2.5 \times 2.5 \times 8 \text{ mm}^3$.

TABLE I
Basic characteristics of the crystals.

Mark	c_{2+} [m ppm]		Origin
	Melt	Crystal	
T. 7718	10^2	4.52	Research Laboratory of Crystal Physics, HAS, Budapest
T. 100	3×10^2	10.41	
T. 2	10^3	38.20	
T. 1.7	10^3	73.34	Inst. of Physics, SAS, Bratislava
T. 6.0	10^3	$\gg 180$	our laboratory

2.2. ITC technique

The measurements have been performed according to the original procedure [1] employed in an extended temperature range (77–393 K). The different steps that make an ITC experiment complete are as follows:

- At a polarization temperature T_p , where the dipolar defect of interest has a short relaxation time $\tau(T_p)$, an electric field E_p is applied to the crystal. The polarization time t_p is chosen so that $t_p \geq \tau(T_p)$, and the saturation-polarization is achieved.
- The temperature of the crystal is lowered to a sufficiently low value T_f when $\tau(T_f)$ will be very large in comparison with the time required for the experiment, and the polarization will be "frozen-in".
- The crystal is kept at T_f so that the fast polarizations may decay isothermally; it is then heated at a linear rate (b). The relaxation time of the dipoles will become shorter and shorter and they will get oriented; hence, a depolarization current results.

The dipolar current i was detected by a vibrating reed electrometer (Cary 31 V), and currents as low as 10^{-16} A were measured. The arrangement employed for plastically deformed samples was described elsewhere [3].

2.3. Relaxation parameters

The relaxation parameters, obtainable from the dipole band, were calculated according to the following estimations:

1. The activation energy E was determined by methods employing the shape parameters of this band, according to [12]:

$$E_i = c_i(kT_m/i) - b_i(2kT_m)$$

with $i = \alpha, \delta, \omega$, where $\alpha = T_m - T_1$, $\delta = T_2 - T_m$, $\omega = T_2 - T_1$, and:

$c_i = c_\alpha = 1.51$ and 1.81 ;	$b_i = b_\alpha = 1.58$ and 2.0 ,
$c_\delta = 0.976$ and 1.71 ;	$b_\delta = 0.0$ and 0.0 ,

$$c_\omega = 2.52 \text{ and } 3.54; \quad b_\omega = 1.0 \text{ and } 1.0$$

for the first- and second-order kinetics, respectively. An empirical way to deal with intermediate cases is a "general order" kinetics which satisfactorily explains the occurrence of various symmetry factors $\mu = \delta/\omega$. It should be noted that the ω approximation is expected to yield the best estimation of E_i for intermediate cases, the α approach should be the best one for bands accompanied by some high-temperature satellites, whereas the δ estimation applies strictly only for the pure first-order bands.

2. Independently of the particular approximation used for the estimation of the activation energy, the inverse frequency factor τ_0 can be calculated from the following equation describing the condition for the band maximum:

$$(bE_i)/(kT_m^2) = (1/\tau_0)\exp(-E_i/kT_m),$$

where b is the heating rate, in our experiments being equal to 0.1 K s^{-1} .

3. The area S under the depolarization curve gives the concentration of dipoles, i.e.:

$$S = \int_T^\infty i(T)dT = N_d g(E_p p^2)/(kT_p)$$

valid for $kT_p \gg E_p p$ and $t_p \gg \tau(T_p)$. The geometrical factor g is related to the possible dipole orientation in the electric field (for AH:Me²⁺ systems $g = 1/3$; E_p , t_p and T_p are the polarization parameters, p — the dipole moment, and k — the Boltzmann constant; $p = ea$ with e denoting the elementary charge and a — the distance between impurity and cation vacancy. For the nearest neighbour (nn, $\langle 110 \rangle$) dipoles $a = (A/2)\sqrt{2}$ with A denoting the lattice parameter, i.e. the cation-cation distance; for instance, for the nnn dipoles $a = A$ and hence $p_{\langle 110 \rangle} = p_{\langle 100 \rangle}/\sqrt{2}$ and $N_{\langle 110 \rangle} = 2N_{\langle 100 \rangle}$.

3. Results and discussion

3.1. Low-temperature range

3.1.1. Experimental data

Some conventional ITC measurements have been performed for plate-shaped samples in the temperature range between 77 and 373 K. The spectra obtained for crystals of various origin were qualitatively similar to each other but clearly different from the spectrum detected for Czochralski's crystals [13]. The main difference concerns the fact that the latter crystals always exhibited the presence of a "Suzuki band" positioned near RT.

Figure 1 presents typical ITC spectra obtained for a sample containing > 180 mole ppm of nickel in the AR and ST state, and polarized at different T_p . Analysis of the low-temperature part of these spectra revealed that:

- For the AR state the dipole band (A) is extremely small.
- The solution treatment of AR samples in air atmosphere results in the appearance of a narrow "H₂O band" which accompanies the dipole band peaking at 202.5 K.

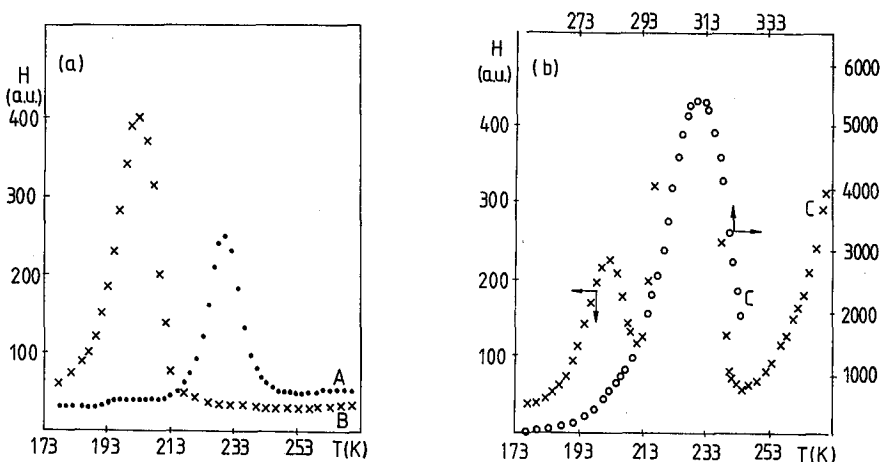


Fig. 1. ITC spectra of AR (curve A) and ST (curves B, C) samples containing more than 180 mole ppm of Ni^{2+} ; part (a) and (b) presents the low-temperature and entire temperature range, respectively. Polarization conditions (T_p [K], T_f [K], V_p [V]): (252, 178, 1900), (221, 178, 1900) and (293, 178, 950) for curves (A), (B) and (C), respectively.

- By lowering the polarization temperature below 238 K the overlapping of both above mentioned bands can be avoided.
- The shape of the dipole band depends neither on the thermal treatment nor on the dopant concentration.
- The band intensity H^A is a linear function of the electric polarization field E_p .
- The value of H^A increases not only during thermal treatment but also with the concentration of the dopant.

The relatively weak dipole band and the linearity of the $H^A(E_p)$ dependence are consistent with dielectric relaxations induced by low concentration of non-interacting dipoles. On the other hand, the relatively low-temperature position of this band T_m^A suggests a contribution of some reorientation mechanisms different from those typical of large dopant ions. Alternatively, one can expect that the dipoles present are not only of nearest-neighbour (nn) but also of next-nearest-neighbour (nnn) type. In order to find the determining parameters it seems necessary to perform the EPR measurements, for instance.

3.1.2. Relaxation parameters

Table II collects the relaxation parameters obtained by using Chen's approximations [12].

According to the estimates of the symmetry parameter the data obtained for the samples T.100, T.6.0 and T.1.7 agree with a pure first-order molecular kinetics of the disorientation process, for which $\mu_g \approx 0.42$ and $\alpha \approx 1.5\delta$. The shape of the dipole bands obtained for T.7718. crystals is "in the middle" between those characteristic of the first- and second-order kinetics; in the latter case $\mu_g \approx 0.52$

and $\alpha = \delta$. For T.2. samples the second-order kinetics is probably dominating; in principle, one should suppose that the dipoles react with more than one relaxation frequency. Unfortunately, the determining parameters are unknown for this series of data.

TABLE II
The relaxation parameters, calculated acc. to R. Chen. [12]

Sample	Quantity	$\omega = T_2 - T_1$	$\alpha = T_m - T_1$	$\delta = T_2 - T_m$	$\mu_g = \delta/\omega$
7718	1) i [K]	15.0	8.0	7.0	0.46
	2) E_i [eV]	0.562	0.615	0.495	
	3) τ_0 [s]	7.20×10^{-13}	3.11×10^{-14}	3.66×10^{-11}	
100	(1)	15.0	8.5	6.5	0.43
	(2)	0.562	0.576	0.533	
	(3)	7.22×10^{-13}	3.17×10^{-13}	3.85×10^{-12}	
2	(1)	17.0	8.5	8.5	0.50
	(2)	0.492	0.576	0.408	
	(3)	4.56×10^{-11}	3.12×10^{-13}	6.56×10^{-9}	
1.7	(1)	14.0	8.0	6.0	0.43
	(2)	0.604	0.615	0.578	
	(3)	5.87×10^{-14}	2.80×10^{-13}	3.11×10^{-14}	
6.0	(1)	15.5	9.0	6.5	0.42
	(2)	0.543	0.541	0.533	
	(3)	2.24×10^{-12}	2.50×10^{-12}	3.85×10^{-12}	

On the other hand, taking into account the approximations made in the above calculations, the average value of the activation energy obtained (0.557 eV) agrees reasonably with the value expected for a d -electron divalent cation. In Fig. 2 $E_i(r_{2+})$ data for NaCl and KCl matrixes are shown, whereas Table III collects the relaxation parameters characteristic of divalent nickel in some alkali halides.

TABLE III
Reorientation parameters characteristic of Ni^{2+} dipoles
in some alkali halides.

Matrix	r_+ [Å]	A [Å]	T_m [K]	E [eV]	τ_0 [s]	Reference
LIF	0.60	4.017	196.5	0.62	-	[14]
NaCl	0.95	5.628	202.5	0.56; (0.65)	8.26×10^{-13}	here; ([2])
KCl	1.33	6.280	189.0	0.49	3.84×10^{-12}	[15]

It is clear that the lattice itself also plays an essential role in determining the jumps of those vacancies which accompany the small impurity ion.

It should be noted that studies of the migration process of divalent nickel in NaCl crystals yield extremely low value for the migration energy [16]. It may be expected that the small value of the reorientation activation energy obtained, and hence the relaxation rates, with which the I.V. dipoles change their orientation under the influence of an electric field, are dominated by the frequency of direct interchange between the Ni^{2+} ion and the cation vacancy.

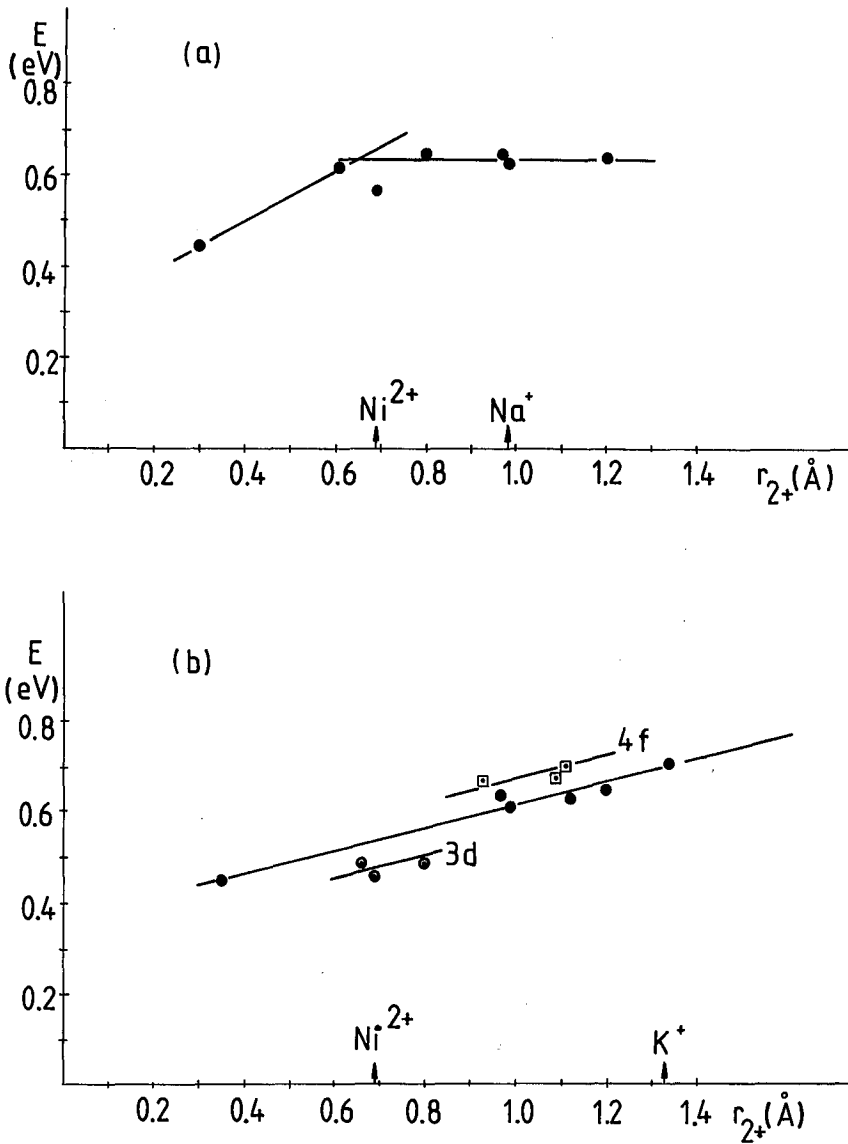


Fig. 2. Activation energy for reorientation of I.V. dipoles in NaCl (a) and KCl (b) crystals as function of the dopant ionic radius.

3.1.3. Concentration of dipoles

Table IV lists the concentration of I.V. dipoles calculated for the nn coordination.

TABLE IV
Comparison of the impurity and dipole concentrations.

	T.7718	T.100	T.2.1	T.1.7	T.6.0
c_{2+}	4.52	10.41	38.20	73.34	$\gg 180$
nn/AR	—	0.6	0.9	2.5	24
nn/ST	4.5	6.7	23.0*	38.0	103
c_{IV}/c_{2+}	≈ 100	≈ 64	≈ 60	≈ 51.8	—

*) or 28 ppm of nn and 10 ppm of nnn dipoles.

It should be noted that the second (next) ITC run brings a decrease of the original (quenched-in) amount of I.V. dipoles which in the average equals 10%. This, rather rapid, decay suggests a low thermal stability of the dipoles considered, and agrees well with their absence in practically all AR samples.

The comparison of the N_d values with the dopant concentrations leads to the conclusion that only a part of the dopant forms isolated I.V. dipoles. The remaining portion of ions is probably present in the form of some aggregates and/or vacancy-rich precipitates. An alternative explanation of this difference may be as follows. Assuming that 100% of the dopant ions is in the form of isolated dipoles, but only part of them takes the nn configuration, the remaining one has been calculated as that corresponding to the nnn configuration. It has been found that the nn/nnn ratio is practically the same for all crystals studied. A similar result was also obtained for the NaCl:Mn²⁺ crystals for which both types of dipoles have been evidenced spectroscopically [17].

3.2. High-Temperature phenomena

3.2.1. Basic data

For AR samples the main features of the high-temperature band are, in principle, similar to those detected for other divalent impurities [3]. Namely, the amplitude H^C and the band location T_m^C are increasing functions of the crystal thickness X , and for a fixed X the value of T_m^C does not depend upon the polarization conditions (T_p , t_p and E_p). Similar to the dipole band H^C is linear with the applied electric field E_p . Both quantities, i.e. H^C and T_m^C , are independent of the material of electrodes used, suggesting that the origin of this band is not related with the injection of some excess charges. On the other hand, however, the dependence of H^C and T_m^C upon X suggests that in addition to the polarization a conductivity contribution should be considered.

Similar to the results obtained previously for much larger impurities [3], the basic features of this band are typical of a dipolar process rather than of a space charge accumulation, for instance. The dislocations surrounded by the impurity clouds in a fashion of the Cottrell atmospheres, could be responsible for a Maxwell-Wagner-Sillars (M-W-S) type interfacial relaxation [4]. Taking into account the currently accepted structure of grown-in dislocations in non-conducting

crystals, their dielectric behaviour may be considered as a sum of two components; namely, a dipolar component, related with relative displacements of the Cottrell clouds around the dislocation core, should be accompanied by a purely ohmic one related with the enhanced pipe diffusion along the dislocation core.

The special role of dislocations surrounded by impurities was evidenced by studying the effect of the dopant concentration and dispersion state as well as the effect of plastic deformation upon the basic characteristics of the band considered.

3.2.2. Effects of the dopant and plastic deformation

For AR samples H^C and T_m^C are increasing functions of c_{2+} , (Fig. 3). It has been stated that the effect of nickel concentration upon T_m^C is the largest from among the divalent impurities studied previously [3]. On the other hand, the lack of saturation of the $H^C(c_{2+})$ relationship resembles the phenomenon of dislocation decoration, when the binding energy between the impurities themselves is larger than their interactions with the dislocation lines. In contrast to the classical Cottrell atmosphere, the "decorated dislocation" can collect an unlimited number of impurities in the form of segregated clusters.

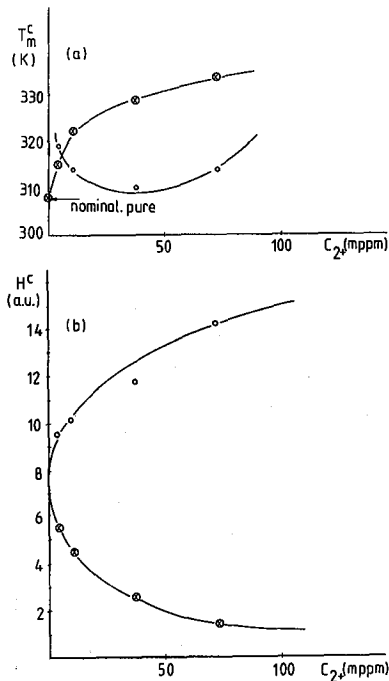


Fig. 3. Effect of the nickel concentration upon some parameters of the high-temperature band in AR (o) and ST (\otimes) samples; parts (a) and (b) present the effect for H^C and T_m^C , respectively.

To modify the state of aggregation of the impurity-related defects, the sam-

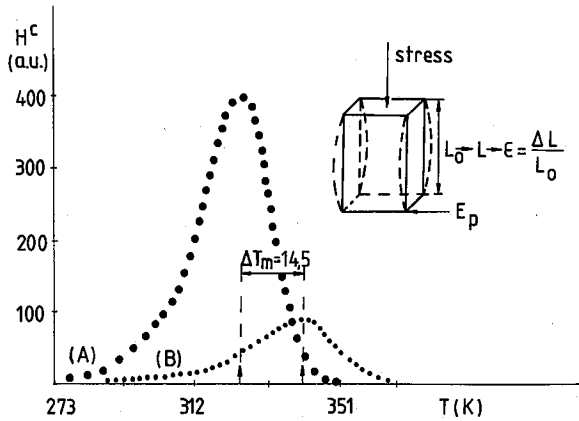


Fig. 4. Effect of plastic deformation upon the high-temperature band for the AR crystal containing 37.0 mole ppm of Ni^{2+} ; curves (A) and (B) correspond to $\epsilon = 0$ and 3.72%, respectively.

ples were subjected to high-temperature annealing. The main effect of this treatment was the shift of T_m^C towards lower values which is understandable in terms of dissolution of the occlusions originally distributed around the dislocation lines.

As a consequence of the changed dislocation density the band intensity H^C drastically decreases and the location of its maximum T_m^C shifts towards higher temperatures. Figure 4 shows the data obtained for a sample containing about 37.0 m ppm of the dopant. It has been found that the value of $\Delta T_m^C = T_m^C(\epsilon) - T_m^C(0)$ is an increasing function of plastic deformation ϵ for each dopant level c_{2+} , and for a given ϵ — it is concentration dependent. In frames of the proposed M-W-S model, the changes of H^C can be understood in terms of the increasing number of imperfections which are introduced into the crystal during plastic deformation. Moreover, the $H^C(\epsilon)$ value depends upon the time t_{an} elapsed at RT between deformation and the ITC test. For instance, 60% of H^C of a sample deformed up to 2.4% recovers after about 16 h. The recovering process may be approximated by a t_{an}^n law with $n \approx 0.4$ resembling the law predicted theoretically for drift of the impurities towards dislocations [18] accompanied by the Ostwald ripening [19].

4. Concluding remarks

1. Ionic thermocurrent data indicate for the AH:Ni^{2+} crystals quite a continuous variation in the reorientation parameters (E_i and τ_0) as well as in the location of the dipole band maximum (T_m^A) with the lattice parameter of the AH matrixes.

2. The reorientation-activation energy E_i , characteristic of the NaCl:Me^{2+} systems, depends on the ionic radius of the dopant r_{2+} in a way similar to the

KCl:Me²⁺ crystals; for both matrixes $r(\text{Ni}^{2+})$ is much smaller than the ionic radius of the matrix cation.

3. The value of the (c_{1V}/c_{2+}) ratio is for the ST samples nearly concentration independent. Hence, it seems reasonably to consider a contribution of nnn dipoles here, whereby the nn and nnn vacancy sites should have almost the same depths, resembling the situation in other Ni²⁺ — doped alkali halides.

4. Examinations of the EPR-signal anisotropy should yield the confirmation of the conclusions given above.

Acknowledgments

The authors wish to thank Mrs. M. Szmida for the technical assistance.

References

- [1] C. Bucci, R. Fieschi, G. Guidi, *Phys. Rev.* **148**, 816 (1966).
- [2] R. Capelletti, *Defects in Solids*, ed. A.V. Chadwick and M. Terenzi, Plenum Publishing Co., London 1986, p. 707.
- [3] M. Suszyńska, R. Capelletti, *Cryst. Res. Technol.* **19**, 1385, 1489 (1984); *Cryst. Res. Technol.* **20**, 1363 (1985).
- [4] V. Daniel, *Dielectric Relaxation*, Acad. Press, London 1967.
- [5] W. Hayes, J.P. Pilbrow, L.M. Slifkin, *J. Chem. Phys. Solids* **25**, 1417 (1964).
- [6] C. Bucci, *Phys. Rev.* **164**, 1200 (1967).
- [7] W. Dreyfus, *Phys. Rev.* **121**, 1675 (1961).
- [8] W. Dreyfus, R.B. Laibowitz, *Phys. Rev.* **148**, 816 (1966).
- [9] F. Agullo-Lopez, J.M. Calleja, F. Cusso, E. Jaque, F.J. Lopez, *Prog. Mater. Sci.* **30**, 187 (1986).
- [10] R. Voszka, J. Tarjan, L. Berkes, J. Krajsovsky, *Krist. Tech.* **1**, 423 (1966).
- [11] D. Nowak-Woźny, M. Suszyńska, *Cryst. Res. Technol.*, (in print).
- [12] R. Chen, *J. Appl. Phys.* **40**, 570 (1969); *J. Mater. Sci.* **11**, 1521 (1976).
- [13] G. Benedek, J.M. Calleja, R. Capelletti, A. Bretschwerdt, *J. Phys. Chem. Solids* **45**, 741 (1984).
- [14] R. Capelletti, M.G. Bridelli, M. Friggeri, G. Ruani, I. Foldvari, L. Kovac, A. Watterich, in *Proc. 5th Symp. Electrets, Heidelberg 1985*, IEEE, New York 1985, p. 294.
- [15] A. Brun, P. Dansas, *J. Phys. C* **7**, 2593 (1974).
- [16] P. Suptitz, J. Teltow, *Phys. Status Solidi* **23**, 9 (1967).
- [17] G.D. Wattkins, *Phys. Rev.* **113**, 79, 91 (1959).
- [18] A. H. Cottrell, A.B. Bilby, *Proc. Phys. Soc. A* **62**, 49 (1949).
- [19] J.M. Lifshitz, V.V. Slezow, *J. Phys. Chem. Solids* **19**, 35 (1961).